Measurements of Transient Membrane Potential after Current Switch-Off as a Tool to Study the Electrochemical Properties of Supported Thin Nanoporous Layers

Andriy Yaroshchuk,* Larisa Karpenko, and Volker Ribitsch

Institut für Chemie, Karl-Franzens-Universität Graz, Heinrichstr. 28, 8010 Graz, Austria

Received: September 7, 2004; In Final Form: February 14, 2005

We have studied the potential of chronopotentiometry after current switch-off as a tool for electrochemical characterization of thin supported nanoporous layers. Within the scope of this technique, a thin supported electrochemically active layer is polarized by direct electric current until a steady state is reached. After that, the current is switched-off in a stepwise manner, and the reading of transient membrane potential begins. A linear non-steady-state theory of the method has been developed in terms of a model-independent approach of network thermodynamics. The measurements of transient membrane potential after current switch-off have been carried out in KCl solutions of various concentrations for a commercially available nanofiltration membrane (Desal5 DK). Such membranes consist of micron-thick active (or barrier) nanoporous layers and much thicker (100−200 μm) and coarse-porous supports (the pore size usually is 0.1−5 μm). The reproducibility of the method has been found to be quite reasonable especially in not too dilute electrolyte solutions and at not too short times ($\geq$10 ms). The relaxation measurements have been complemented by the measurements of the steady-state membrane potential and by sample measurements of salt rejection in the pressure-driven mode, which enabled us to carry out a self-consistent interpretation of the experimental data. This has revealed, in particular, that the ion rejection mechanism related to the fixed electric charges is not the dominant one in the case of the Desal5 DK nanofiltration membrane. Proceeding from a quantitative interpretation of relaxation patterns, we could also determine some properties of membrane support, namely, the porosity and the salt diffusivity. They have been found to have reasonable values remarkably independent of salt concentration, which confirms the self-consistency of our interpretations.

Introduction

The electrochemical properties of nanoporous media are important for their interactions with charged solutes such as ions, peptides, proteins, and colloidal particles. The nanoporous media are often used and studied in the form of thin layers deposited on top of much thicker supports, whose principal function is to add mechanical strength and to make the micron-thick layers easier to handle. Therefore, it is desirable to have experimental techniques for the studies of electrochemical properties of thin supported nanoporous layers. The conventional steady-state electrochemical techniques such as membrane potential measurements or the Hittorf method are not informative here because of the usually large contributions of supports to the diffusion resistance of such bilayer systems (see below for a discussion). Information on the properties of thin supported nanoporous layers can be obtained from non-steady-state measurements. As shown below, integrated sets consisting of non-steady- and steady-state measurements are especially informative.

Composite or asymmetric nanofiltration membranes are convenient models of supported thin nanoporous layers. They consist of micron-thick active (or barrier) nanoporous layers and much thicker (100−200 μm) coarse-porous supports (the pore size usually is 0.1−5 μm). The information on the electrochemical properties of active layers is useful for the understanding of rejection mechanisms of nanofiltration and for its modeling.[1]

Electrical capacities in electrolyte solutions charge very rapidly, namely, at characteristic times of diffusion relaxation of diffuse parts of double electric layers. Even in very dilute solutions, that time does not exceed 10^{-6} s. Therefore, for our purposes, the electric current can always be considered continuous, which considerably simplifies the interpretation.

The concentration polarization by electric current of boundaries between layers with different electrochemical properties gives rise to the appearance of the diffusion component of the transmembrane electric potential difference even if there is no external composition difference. This concentration polarization cannot disappear immediately after the current switch-off. The cause for the time lag is the fact that the distributed chemical capacity[2,3] (see below) in the vicinity of the boundary has to "discharge".

The chronopotentiometry after stepwise changes in the polarizing current (both switch-on and switch-off) has been used in refs 4 and 5 to study the polarization of monolayer ion-exchange membranes. Though the basics of the technique used in the present study are the same as in refs 4 and 5, the profound differences in the structure of the membranes (very thin and supported in this study vs relatively thick and monolayer in refs 4 and 5) made the characteristic time scales typical of this study several orders of magnitude shorter than those encountered in refs 4 and 5. That has given rise to considerable differences in the approaches to the data acquisition and treatment. Besides that, the non-steady-state theory devel-

* Author to whom correspondence should be addressed. Present address: Laboratory of Radioactive Waste Management, Paul-Scherrer-Institut, 5232 Villigen PSI, Switzerland. Phone: +41 (0)56 310 5316. Fax: +41 (0)56 310 4595. E-mail: andriy.yaroshchuk@psi.ch.

10.1021/jp040599f CCC: $30.25
Published on Web 03/22/2005

oped in this paper is model-independent (network thermodynamics) while the mechanistic Nernst−Planck approach was used in refs 4 and 5. In refs 6 and 7, the chronopotentiometry has been applied to study the ion transport in bilayer bipolar membranes. Their structure is closer to that of the systems of interest for this study. Nevertheless, the typical thicknesses of layers in bipolar membranes are about 2 orders of magnitudes larger than the thicknesses of active layers of nanofiltration membranes. Accordingly, the relaxation processes studied in refs 6 and 7 were essentially slower than in this study. Besides that, the principal emphasis of refs 6 and 7 was on the differentiation between the reversible and irreversible contributions to the transmembrane potential difference and on the understanding of ion transfer in the so-called overlimiting mode. The latter made the system too complex for the development of a quantitative theory.

This paper is organized in the following way. First, we outline the basic equations of linear non-steady-state theory for the time-dependent distribution of the salt chemical potential in polarized multilayer systems. That theory is developed in terms of network thermodynamics and, thus, operates with model-independent properties such as ion transport numbers, diffusion permeabilities, chemical capacities, etc. In the subsequent interpretation of experimental data, that enabled us to obtain the phenomenological characteristics of thin nanoporous layers without the need to specify any mechanistic model. Further on, the basic equations are specified and solved for the particular case of the electric response of a bilayer system to a stepwise current switch-off.

In the Experimental Section, we briefly describe our test cell as well as the measurement and data acquisition protocols.

In the results and discussion section, a set of statistically representative membrane potential transients is presented and interpreted as obtained from measurements with KCl solutions of various concentrations. Besides that, the results of complementary measurements of the steady-state membrane potential in the same solutions are presented. For the 0.03M KCl solution where data on the salt rejection are also available, a self-consistent interpretation of experimental data is carried out. Further on, under assumption that the properties of the supports are independent of the salt concentration, the same interpretation is carried out for the other salt concentrations used in this study.

Theory

The basic equations of linear non-steady-state theory for the time-dependent distribution of the salt chemical potential in polarized multilayer systems have been derived in ref 8. For a membrane consisting of several macroscopically homogeneous layers, the basic equation for the time-dependent distribution of salt chemical potential, μ, can be written in this dimensionless form

$$\beta_k^{\,2}\frac{\partial\mu}{\partial\tau}=\frac{\partial^2\mu}{\partial\xi^2} \tag{1}$$

where k is the layer index, the transmembrane coordinate is scaled on the active layer thickness, $\xi \equiv x/l_a$, and the dimensionless time, τ, is obtained by scaling time by the diffusion relaxation time of the active layer defined in this way

$$t_0 \equiv \frac{\alpha_a}{\chi_a} l_a^{\,2} \tag{2}$$

where the index a denotes the properties of the active layer and χ_k is the specific diffusion permeability of the kth membrane layer material for the salt. The coefficients β_i are defined in this way

$$\beta_k^{\,2} \equiv \frac{\alpha_k\chi_a}{\alpha_a\chi_k} \tag{3}$$

where α is the so-called specific chemical capacity defined as

$$\alpha \equiv \left(\frac{\partial q_s}{\partial\mu}\right)_{T,P} \tag{4}$$

This is a quantitative measure of how much salt (δq_s) has to be added to a unit volume of a medium to change the salt chemical potential by $\delta\mu$. A detailed discussion of this useful property and its estimates for various media can be found in refs 2 and 3. By definition, $\beta_a \equiv 1$.

One of the boundary conditions to eq 1 is the continuity of salt chemical potential at all the boundaries between the layers (local interfacial equilibria). At zero transmembrane volume flow, the boundary condition for the salt flux can be shown to have this form[8]

$$\chi_k\frac{\partial\mu}{\partial\xi}\bigg|_{\xi=\xi_k} - \chi_{k+1}\frac{\partial\mu}{\partial\xi}\bigg|_{\xi=\xi_k} = \frac{Il_a}{FZ_1\nu_1}\Delta t_1|_{\xi=\xi_k} \tag{5}$$

where ξ_k are the coordinates of the boundaries and $\Delta t_1 \equiv t_1|_{\xi_k-0} - t_1|_{\xi_k+0}$ are the changes of the ion transport number at the boundaries. Thus, the boundaries between the layers with different electrochemical properties are sources of salt flux. Despite the appearance of salt flux sources, electric charges do not arise at the boundaries since exactly as much charge is taken away from the boundary by anions as is brought to it by cations and vice versa.

We shall further consider a bilayer system consisting of a nanoporous layer and a support. Due to vigorous stirring, the salt concentrations (and thus, its chemical potentials) at the external surfaces are the same at any given time. In our experimental setup for the measurements of transient membrane potential, the salt concentrations are the same at both external surfaces. Since the chemical potential is defined up to a constant, its preset constant value at the external surfaces may be taken equal to zero. The model and the chosen coordinates are shown in Figure 1. The boundary conditions for this system are

$$\mu_a(-1,\tau) = 0 \tag{6}$$

$$\mu_s(h,\tau) = 0 \tag{7}$$

$$\mu_a(0,\tau) = \mu_s(0,\tau) \tag{8}$$

$$\chi_a\frac{\partial\mu_a}{\partial\xi}\bigg|_{\xi=0} - \chi_s\frac{\partial\mu_s}{\partial\xi}\bigg|_{\xi=0} = \frac{I(\tau)l_a}{FZ_1\nu_1}\Delta t_1|_{\xi=0} \tag{9}$$

where indices a and s denote the nanoporous layer and support, respectively, and $I(\tau)$ is the current density as a function of time. The solution to eq 4 is sought in this form (Fourier transform)

$$\mu_i(\xi,\tau) \equiv \frac{1}{2\pi}\int_{-\infty}^{+\infty} d\omega\, \exp(-i\omega\tau) f_i(\xi,\omega) \tag{10}$$

where ω is the dimensionless circular frequency (scaled on $1/t_0$) and $f_i(\xi,\omega)$ is the complex spectral density of temporal response.

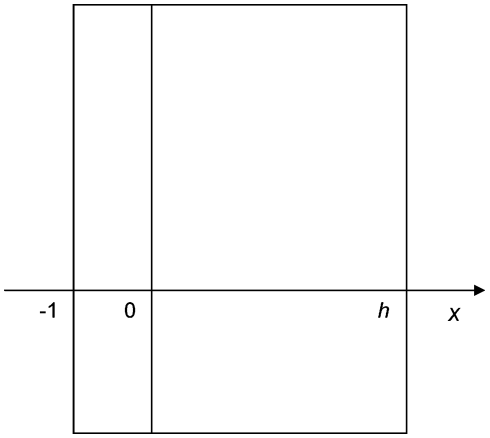

Figure 1. Model.

By substituting eq 10 into eq 4, we obtain these fundamental solutions

$$f_i^{(\pm)}(\xi,\omega) \equiv \exp\left(\pm(1-i)\beta_i\sqrt{\frac{\omega}{2}}\xi\right) \tag{11}$$

Accordingly, the general solutions for the spectral densities have this form

$$f_i(\xi,\omega) = A_i^{(+)}\exp\left((1-i)\beta_i\sqrt{\frac{\omega}{2}}\xi\right) + A_i^{(-)}\exp\left(-(1-i)\beta_i\sqrt{\frac{\omega}{2}}\xi\right) \tag{12}$$

where $A_i^{(\pm)}$ are the integration constants.

By applying the boundary conditions, we obtain a system of equations for the integration constants that can be solved to yield for the spectral density of difference of salt chemical potentials across the active layer[9] $R(\omega)$

$$R(\omega) = \frac{S(\omega)}{\coth\left((1-i)\sqrt{\frac{\omega}{2}}\right) + r\coth\left((1-i)b\sqrt{\frac{\omega}{2}}\right)} \tag{13}$$

where we have denoted

$$r \equiv \sqrt{\frac{\alpha_s\chi_s}{\alpha_a\chi_a}} \tag{14}$$

$$b \equiv \beta_s h \tag{15}$$

$$S(\omega) \equiv \frac{I(\omega)}{FZ_1\nu_1}\Delta t_1\left(\frac{l_a}{\chi_a}\right)\frac{1+i}{\sqrt{2\omega}} \tag{16}$$

Here, $I(\omega)$ is the Fourier transform of $I(\tau)$. If the current is switched-off in a stepwise manner (which is the case in our experiments), then its Fourier transform is

$$I(\omega) = I_0\left(\pi\delta(\omega) - \frac{i}{\omega}\right) \tag{17}$$

It can be shown that at zero electric current (i.e., after the current switch-off), the difference in the electric potentials between the half-cells separated by a polarized bilayer system for (1:1) electrolytes is related to the difference in the salt chemical potentials across the active layer in this way

$$E_m(\tau) = \frac{2\Delta t_1}{F}\Delta\mu_a(\tau) \tag{18}$$

By substituting eqs 13, 16, and 17 into eq 18 and by taking the real part for the chronopotentiometric response, we obtain this

$$E_m(\tau) = \frac{I_0(\Delta t_1)^2}{F^2}\left(\frac{l_a}{\chi_a}\right)\left(\frac{1}{1+\rho^{-1}} + \mathrm{Re}\left(\frac{1-i}{\pi}\int_{-\infty}^{+\infty}\frac{d\omega}{\omega\sqrt{2\omega}}\times \frac{\exp(-i\omega\tau)}{\coth\left((1-i)\sqrt{\frac{\omega}{2}}\right) + r\coth\left((1-i)b\sqrt{\frac{\omega}{2}}\right)}\right)\right) \tag{19}$$

where we have denoted

$$\rho \equiv \frac{b}{r} \equiv \frac{\chi_a}{\chi_s}h \tag{20}$$

The last parameter is equal to the ratio of molar diffusion permeabilities of the nanoporous layer and the support.

From the definitions of chemical capacity (eq 3) for ideal solutions, one can obtain

$$\alpha = \frac{c_s}{RT}\left(\Gamma_i + c_s\frac{d\Gamma_i}{dc_s}\right) \tag{21}$$

where c_s is the salt concentration and Γ_i is the distribution coefficient (including the medium porosity, if applicable) of the ith ion between the medium of interest and the equilibrium electrolyte solution. Since there is no accumulation of electric charge anywhere within the membrane,[10] cations and anions are added (or withdrawn) in stoichiometric quantities. Therefore, the chemical capacity can be defined for any of the ions. In ion-exchange media in equilibrium with dilute electrolyte solutions, the distribution coefficient of co-ions is small.[11] The second term in parentheses in eq 21 can be shown to be of the same order of magnitude as the first one. Therefore, the specific chemical capacity of ion exchangers is essentially smaller than that of bulk electrolyte solutions (the latter is simply equal to c_s/RT). From that, the definition of the parameter r (eq 14), and the physics of diffusion permeabilities, it follows that in the case of relatively dense (and probably electrochemically active) nanoporous layers flanked by relatively loose supports, the parameter r may be fairly large.[12] In this case, it is useful to introduce a new characteristic relaxation time according to

$$t_0^* \equiv t_0 r^2 \tag{22}$$

If a new dimensionless time is introduced as $\tau^* \equiv t/t_0^*$, eq 19 can be written in this form

$$\tilde{E}_m(\tau^*) = \frac{2\tilde{I}_0(\Delta t_1)^2}{P_a + P_s}\left(1 + \left(1+\frac{1}{\rho}\right)\mathrm{Re}\left(\left(\frac{1-i}{\pi}\right)\int_{-\infty}^{+\infty}\frac{d\omega}{\omega\sqrt{2\omega}}\times \frac{\exp(-i\omega\tau^*)}{\coth\left((1-i)\rho\sqrt{\frac{\omega}{2}}\right) + \frac{1}{r}\coth\left((1-i)\frac{1}{r}\sqrt{\frac{\omega}{2}}\right)}\right)\right) \tag{23}$$

where $\tilde{E}_m \equiv FE_m/RT$ is the dimensionless transmembrane electric potential difference, the reduced current density $\tilde{I}_0$ is

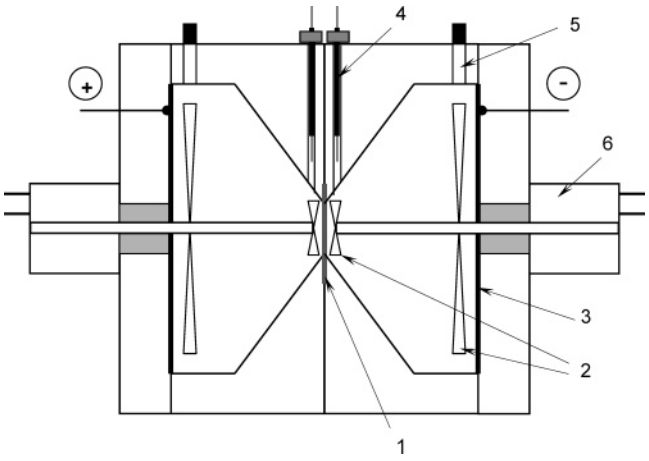

Figure 2. Test cell: (1) membrane sample; (2) propeller-like stirrers; (3) polarizing disk-shaped Ag/AgCl electrodes; (4) indicator Ag/AgCl electrodes; (5) openings for the solution delivery; (6) motors.

defined as $\tilde{I}_0 \equiv I_0/2Fc_s$, and $P_{a,s} \equiv (RT/c_s)(\chi_{a,s}/l_{a,s})$ are the molar diffusion permeabilities of nanoporous layer and support, respectively. With eq 23, it is easy to consider the limiting case of very large r. Indeed, when $r \rightarrow \infty$, eq 23 reduces to

$$\tilde{E}_m(\tau^*) \xrightarrow[r\to\infty]{} \frac{2\tilde{I}_0(\Delta t_1)^2}{P_a + P_s}\left(1 + \frac{1}{\pi}\left(1 + \frac{1}{\rho}\right) \times \right.$$
$$\left. \mathrm{Im}\left(\int_{-\infty}^{+\infty} \frac{d\omega}{\omega} \frac{\exp(-i\omega\tau^*)}{1 + (1-i)\sqrt{\frac{\omega}{2}}\coth\left((1-i)\rho\sqrt{\frac{\omega}{2}}\right)}\right)\right) \quad (24)$$

Since parameter r enters into the definition of the characteristic relaxation time of eq 22, the dependencies plotted against the dimensional time would still depend on r. However, in a logarithmic scale its variation would only cause their shift along the time axis without a change of shape. That simplifies the interpretation considerably, so it is important to know what values of the parameter r may be considered sufficiently large in this context. Sample calculations have revealed that the accuracy of the approximation of infinitely large r depends on the ratio of layer diffusion permeabilities, ρ. Thus, for instance, when $\rho \rightarrow 0$ (the relaxation controlled by the diffusion through the support), the difference between the relaxation patterns is still noticeable even when $r \geq 30$. When the ratio of diffusion permeabilities of layers increased, the situation improved, and already at $\rho = 0.5$, the dependence of the shape of transients on parameter r practically disappeared at $r \geq 10$. As follows from the experimental data presented below, the limiting case $\rho \rightarrow 0$appears to be rather unrealistic for the membrane used in this study. Therefore, in the interpretation of experimental data, we shall use the limiting case $r \rightarrow \infty$ and check the value of this parameter a posteriori.

Experimental Section

Methods. All of the measurements have been carried out in a two-compartment test cell schematically shown in Figure 2. The membrane was polarized by a pair of disk-shaped Ag/AgCl electrodes with a large area. The membrane area was 1.13 cm^2. Vigorous stirring was ensured by propeller-like stirrers located parallel to the membrane surface and driven by external motors. Another pair of stirrers was located near the current-supply electrodes to diminish their polarization. The transmembrane potential difference was measured by a pair of bare Ag/AgCl electrodes. Since our measurements have been carried out after the current switch-off (i.e., at zero electric current), in principle, each of the indicator electrodes could be located anywhere in the corresponding half-cell. However, in test measurements without the membrane, we have noticed that when the electrodes were exposed to the current during the polarization, some poorly reproducible responses to the current switch-off occurred. We have interpreted that as a result of current passage through the unisolated tips of the Ag/AgCl electrodes. Due to the corresponding concentration polarization, a local distribution of the electrolyte concentration developed in the vicinity of each electrode. Because of inevitable differences in the shape of the electrodes and in the hydrodynamic conditions in their vicinity, those distributions could not be identical, hence a transient potential difference. The phenomenon disappeared when the electrodes were receded into the corresponding bores so that they were not exposed to the current.

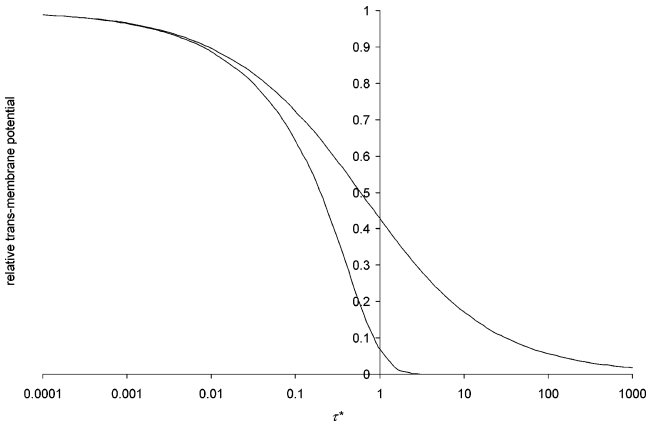

Figure 3. Transmembrane potential scaled on the initial value against dimensionless time, τ^*, $r \rightarrow \infty$: $\rho \rightarrow 0$ (left curve); $\rho \rightarrow \infty$ (right curve).

The whole test cell was enclosed in a Faraday cage, and all of the cables were thoroughly screened. The data acquisition was performed by a personal computer with the aid of dedicated software.

Materials. The membrane was a commercially available Desal5 DK (polyamide, composite on a polysulfone support). The electrolyte was KCl of various concentrations. The pH value was kept at 5.6. The membranes were equilibrated with working solutions overnight.

Results and Discussion

It can be shown that the interpretation of steady-state voltammetry of nanofiltration membranes is complicated by rather large ohmic contributions (most probably due to relatively high electrical resistances of membrane supports). The technique of chronopotentiometry of membrane potential after current switch-off has been developed primarily to eliminate the ohmic contributions. After the current switch-off, they vanish almost immediately, and one can observe unobstructed the temporal evolution of the transient membrane potential, which is often almost 2 orders of magnitude smaller than the values occurring at nonzero currents for this kind of membranes and for our cell configuration.

Figure 3 shows two relaxation patterns calculated at $r \rightarrow \infty$ for the limiting modes of nanoporous-layer-controlled ($\rho \rightarrow \infty$) and support-controlled ($\rho \rightarrow 0$) relaxation. It is seen that in the former case the dispersion is essentially broader. It can be shown that in terms of shape the relaxation patterns corresponding to the intermediate (mixed) modes are always situated between those two extremes. Thus, for the interpretation of relaxation patterns, it is important to have information on the ratio of

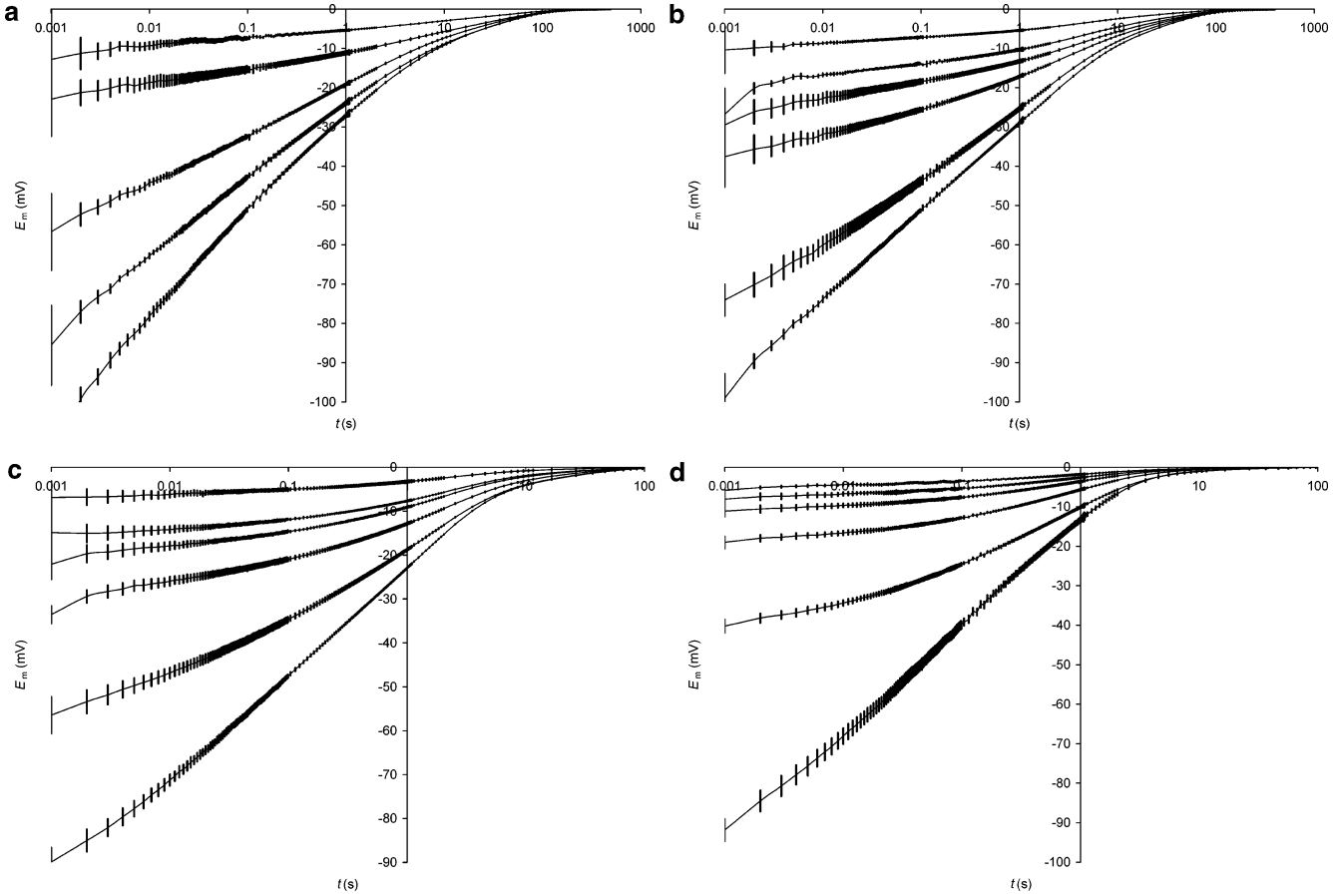

Figure 4. Transients of transmembrane potential obtained in KCl solutions of pH 5.6 (membrane area 1.13 cm^2): (a) $c_s = 0.001$ M, current = 0.01, 0.02, 0.04, 0.05, 0.07 mA (from top to bottom); (b) $c_s = 0.003$ M, current = 0.04, 0.067, 0.08, 0.1, 0.15, 0.167 mA (from top to bottom); (c) $c_s = 0.01$ M, current = 0.2, 0.4, 0.5, 0.6, 0.8, 1.0 mA (from top to bottom); (d) $c_s = 0.03$ M, current = 1.0, 1.5, 2.0, 3.0, 5.0, 7.0 mA (from top to bottom).

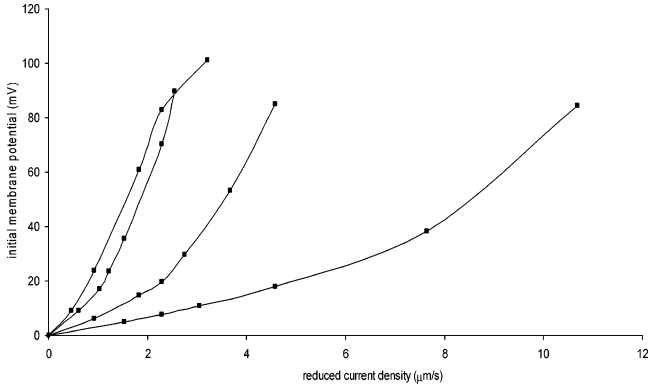

Figure 5. Transmembrane potential measured at 2 ms after the current switch-off against reduced current density current; pH 5.6; $c_s = 0.001$, 0.003, 0.01, 0.03 M (from left to right).

diffusion permeabilities of layers. As shown below, this ratio also essentially controls the steady-state membrane potential (see also ref 13) and, thus, may be determined from it.

Figure 4 shows the transients of transmembrane potential obtained in KCl solutions of several concentrations. Each curve has been obtained by averaging at least five measurements. The method is well reproducible. At lower currents, the curve shape is in accordance with the theoretical shape. At higher currents, however, there is a noticeable quantitative deviation from theory.

Figure 5 shows the values of the transmembrane potential measured at 2 ms after the current switch-off as functions of polarizing current density. It is seen that after initially linear behavior the experimental plots become superlinear. At the same time, the experimental voltage does not go to infinity at a limiting current but just increases more rapidly starting from a certain current range. This phenomenon has also been observed for the classical steady-state voltammograms with various membranes[14] and is usually referred to as overlimiting current. Typically, its occurrence is explained in terms of contributions to the current transfer of hydrogen and hydroxyl ions arising due to water dissociation.

TABLE 1: Steady-State Membrane Potential Measured in KCl Solutions (pH 5.6) at a Concentration Ratio of 2[a]

concentration (kmol/m^3)	E_{ms} (mV)
0.001	5.94 ± 0.31
0.003	5.16 ± 0.4
0.01	2.35 ± 0.33
0.03	1.12 ± 0.22

[a] Indicated are the concentrations at the active membrane side; the concentrations at the support side were 2 times lower.

In Figure 5, the last two plots to the left are quite close to each other, which indicates an increasing relative contribution of diffusion through the support with decreasing salt concentration. This interpretation is confirmed below by the estimates of layer diffusion permeabilities (Table 2).

By using eq 23 for the initial value of the transmembrane electric potential immediately after the current switch-off, one can obtain this

$$\frac{\tilde{E}_{mi}}{\tilde{I}} = 4\frac{(t_a - t_s)^2}{P_a + P_s} \qquad (25)$$

TABLE 2: Estimated Values of Cation Transport Number and Diffusion Permeability of the Active Layer against Salt Concentration

c_s (kmol/m^3)	t_a	P_a (μm/s)	$\rho \equiv P_a/P_s$
0.001	0.874	0.26	0.6
0.003	0.823	0.25	0.6
0.01	0.823	1.1	2.4
0.03	0.842	3	6.7

Along with the sought-for difference of ion transport numbers between the active layer and the support,[15] the equation contains the diffusion permeabilities of constituent layers, which are a priori unknown. The information on the diffusion permeability of the nanoporous layer (also called "solute permeability" in this context) can be obtained from the interpretation of pressure-driven salt rejection measured at various transmembrane volume flows.[16] The remaining unknown diffusion permeability of support can be determined in two ways. First, it can be estimated from the steady-state membrane potential by using this expression, which is easy to derive for a bilayer system

$$\tilde{E}_{ms} = \left(2\frac{P_s t_a + P_a t_s}{P_a + P_s} - 1\right)\left(1 - \frac{c_s''}{c_s'}\right) \qquad (26)$$

where $\tilde{E}_{ms}$ is the dimensionless steady-state membrane potential measured for the solutions of concentrations c_s' and c_s'' separated by the bilayer. In the particular case of KCl solutions where $t_s \cong {}^1/_2$, eq 26 reduces to

$$\frac{\tilde{E}_{ms}}{1 - \frac{c_s''}{c_s'}} = \frac{P_s}{P_s + P_a}(2t_a - 1) \qquad (27)$$

Thus, the smaller the relative diffusion permeability of the support, the smaller the steady-state membrane potential. Equations 26 and 27 contain not only the unknown diffusion permeability of support but also the sought-for transport number of counterions in the active layer. Therefore, eqs 25 and 26 should be solved as a system of algebraic equations.

Another possibility is to separately measure the diffusion resistance of the bilayer system as a whole. In this case, evidently

$$P_m^{-1} = P_a^{-1} + P_s^{-1} \qquad (28)$$

where P_m is the diffusion permeability of the bilayer system. The first option is more accurate when the diffusion permeability of the support is high, while the second one is preferable when it is low (and the support, accordingly, makes a relatively large contribution to the total diffusion resistance). An advantage of the first option is that the measurements of the steady-state membrane potential can be carried out in the same cell used for the chronopotentiometry measurements, while for the diffusion measurements a separate test cell is needed.

Figure 6 shows the rejection of a 0.03M KCl solution (pH 5.6) as a function of the transmembrane volume flow measured with the Desal5 DK membrane by Boiko and Makovetskiy[17] in a batch test cell with a vigorous stirring. The solid line is a modified Spiegler−Kedem fit,[16] from which the following transport properties of the active layer could be estimated $P_a = 3.0$ μm/s, $\sigma_s = 0.79$, and $a = 0.65$, where σ_s is the so-called salt reflection coefficient and a is a semiempirical parameter accounting for the dependence of transport properties of nanoporous layers on the salt concentration.

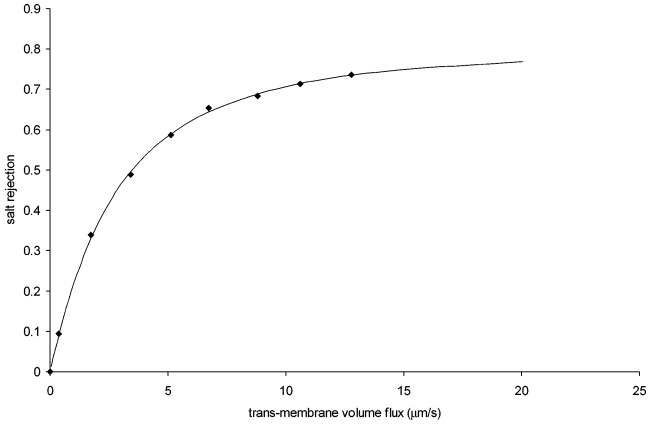

Figure 6. Rejection of 0.03 M KCl solution (pH 5.6) by Desal5 DK membrane as a function of transmembrane volume flow and the modified Spiegler−Kedem fit.[16]

For the same membrane and solution, we have measured a steady-state membrane potential of 1.12 ± 0.22 mV (Table 1). The ratio of initial membrane potential to the polarizing current density was taken from the data shown in Figure 5. That enabled us to estimate the potassium transport number within the active layer at 0.842 and the diffusion permeability of the support at $P_s = 0.45$ μm/s. Since the membrane supports usually have relatively large pores, it is reasonable to assume that their diffusion permeability is not strongly dependent on the salt concentration. Having assumed the diffusion permeability of the supports to be independent of concentration, from the initial membrane potential after the current switch-off, E_{mi}, and the steady-state membrane potential, E_{ms}, (Table 1), we could estimate the values of the cation transport number and the diffusion permeability of the active layer in the solutions of other concentrations used in this study. The results are presented in Table 2. The diffusion permeability decreases with decreasing salt concentration, which is in qualitative agreement with the electrochemical activity of the active layer. However, at the same time, the ion transport number is practically independent of the concentration, which is not consistent with the simple fixed-charge model. Moreover, from the value of the ion transport number, assuming the ratio of the cation and anion mobilities in the active layer to be the same as in the bulk, we could estimate the fixed-charge density and, from it, the salt reflection coefficient, which would occur if the salt rejection was caused by the effect of fixed charge alone. In the 0.03 M KCl solution, that "electrochemical" reflection coefficient was found to be 0.27 while the actual value was 0.79. More representative of the rejection mechanism(s) is the transmission coefficient defined as one minus the reflection coefficient. For the Desal5 DK membrane in 0.03 M KCl solution (pH 5.6), the ratio of the "electrochemical" transmission coefficient to the measured one is equal to 3.5. This means that the principal contribution to the salt rejection is made by a mechanism other than the Donnan exclusion. If we further speculate that this non-Donnan mechanism is, for example, the dielectric exclusion,[18] whose strength is known to essentially decrease with increasing electrolyte concentration, then we may even reconcile the practically constant cation transport number with the strongly varying diffusion permeability of the active layer. The fact is that the dielectric exclusion has a direct effect on the diffusion permeability but not on the ion transport numbers.

The information on the diffusion permeabilities of the membrane layers enables us to carry out a quantitative interpretation of transients of the transmembrane potential. Thus, for instance, in the 0.03 M KCl solution we have estimated ρ

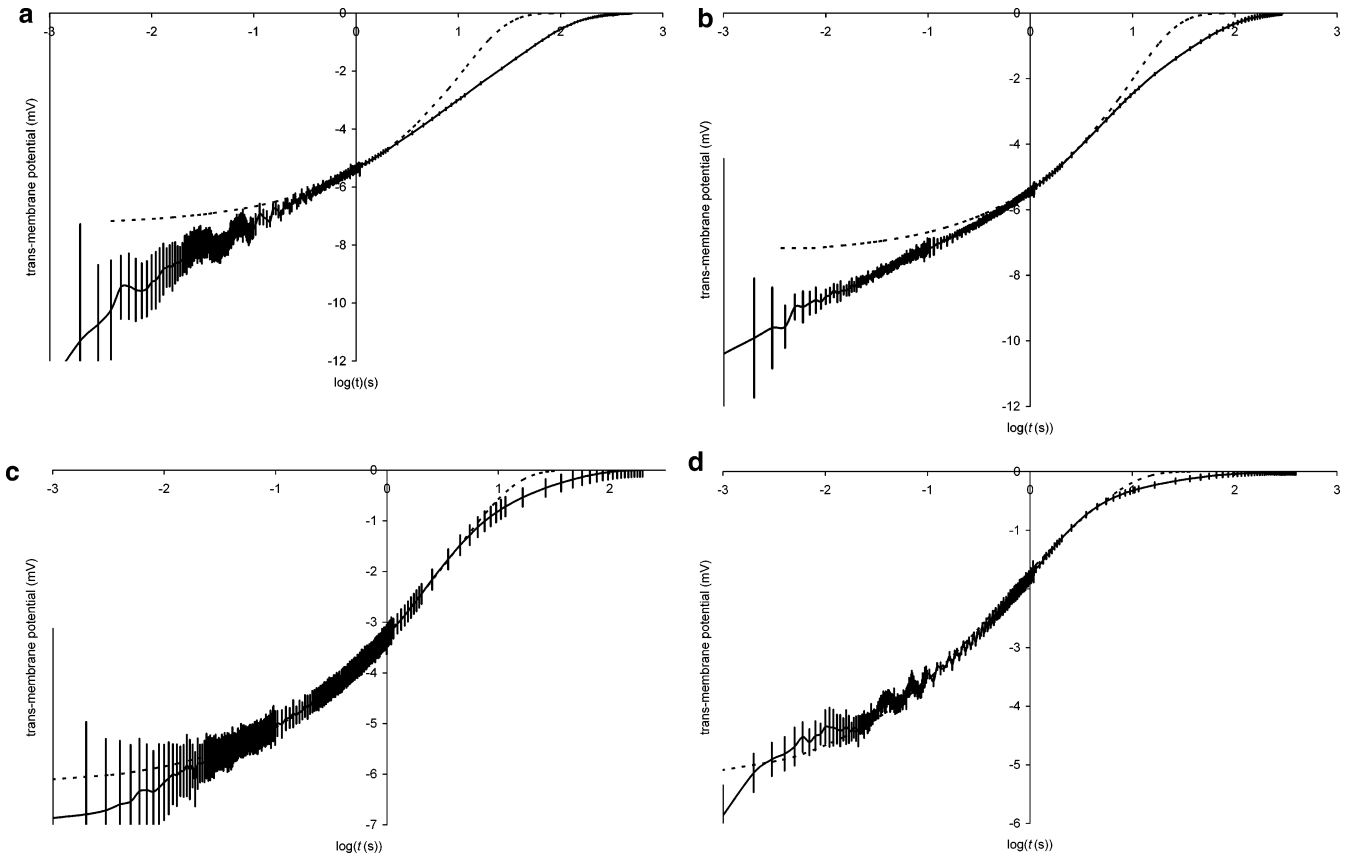

Figure 7. Theoretical fits (dashed lines) of transient transmembrane potentials: (a) $c_s = 0.001$ M, current = 0.01 mA; (b) $c_s = 0.003$ M, current = 0.04 mA; (c) $c_s = 0.01$ M, current = 0.2 mA; (d) $c_s = 0.03$ M, current = 1.0 mA.

TABLE 3: Some Characteristics of Chronopotentiogrammes and the Properties of Constituent Layers Estimated from the Interpretation of Experimental Data[a])

concentration (kmol/m^3)	reduced current density (μm/s)	E_{mi} (mV)	P_a/P_s	t_0^*(s)	γ_s	D_s (10^{-9} m^2/s)
0.001	0.46	−7.3	0.58	123	0.114	0.63
0.003	0.61	−7.35	0.57	112	0.101	0.72
0.01	0.92	−6.25	2.4	5.8	0.096	0.75
0.03	1.53	−5.40	6.7	0.9	0.107	0.68

[a] See text for explanations.

= 6.7. With this parameter known, the theoretical relaxation pattern of eq 22 contains only two unknown values, namely, the initial value of the transmembrane potential right after the current switch-off and the characteristic relaxation time, t_0^*. Figure 7 shows the results of theoretical fits of transients of the transmembrane potential obtained at the lowest polarizing current densities when the linear theory can be applied. The fitted parameters are listed in Table 3. From Figure 7, it is seen that in the more concentrated solutions (0.01 M and, especially, 0.03 M), the fit quality is fairly reasonable. With the decrease in salt concentration, however, ever more pronounced deviations occur, first at the long, then also at the short times.

Though the quality of theoretical fits in the more dilute solutions is poor, it should, nevertheless, be noted that the fits shown in Figure 7 were the only ones coinciding with the experimental data at the intermediate times within, at least, 1 order of magnitude. That may be an indication of the fact that the fitted parameters (especially, the characteristic relaxation time) in this case have some physical meaning and do describe the relaxation process of interest. The deviations may be a consequence of the occurrence of other relaxation processes not included in this simple model of a strictly bilayer system. Thus, for instance, an intermediate layer may well exist between the active layer and the support. The pore size in this intermediate layer is also intermediate. Therefore, it may be that the layer exhibits some electrochemical activity in the more dilute solutions while being practically passive in the more concentrated ones due to the screening of fixed charges by the shrinking diffuse parts of double electric layers. It is also logical to assume that the thickness of the intermediate layer may be essentially larger than that of the active layer. Because of that, the characteristic time of relaxation of the polarization of this layer may well be much longer than that of the principal relaxation process. All that may yield just a very slow relaxation similar to that observed in the more dilute solutions.

As far as the deviations at the short times are concerned, we should remember that the membrane supports often have a complex spongelike structure with many microinterfaces where some changes in the electrochemical properties are quite possible. "Micromembranes" delimited by such interfaces, of course, are polarized by the electric field. The theory developed in this paper is qualitatively applicable to the relaxation processes near such local interfaces as well. In particular, we have seen that the magnitude of the electrical response strongly depends on the electrochemical activity. Besides that, the rate of relaxation strongly increases with the increasing diffusion permeability of electrochemically active layers. If we hypothesize that the micromembranes are rather thin and loose, then their electrochemical activity and diffusion permeability may strongly depend on the salt concentration. Accordingly, in the more concentrated solutions, the magnitude of the electrical response may be too low and the relaxation too rapid for the signal to be observed within the temporal resolution of our experiments. At the same time, the polarization of the micromembrane may well make a noticeable contribution to the total electrical response in the more dilute solutions.

The above reasoning is qualitatively confirmed by the observation that the aforementioned deviations also occurred in the more concentrated solutions at higher densities of polarizing current. The fact is that with increasing current density due to the progressively decreasing concentration near the interface between the active and intermediate (or support) layers the latter is exposed to an ever more dilute salt solution with all of the consequences discussed above.

From the comparison of Table 3 with Figure 5, it is seen that in the more concentrated solutions (0.03 and 0.01 M) the values of the initial membrane potential correspond fairly well to the values measured 2 ms after the current switch-off and shown in Figure 5.

The fitted values of the characteristic relaxation time can be further used to obtain information on the properties of membrane support. Indeed, by using the definitions of characteristic relaxation times of eqs 2 and 22, we obtain

$$t_0^* \equiv \alpha_s \chi_s \left(\frac{l_a}{\chi_a}\right)^2 \equiv \alpha_s \chi_s \left(\frac{RT}{c_s P_a}\right)^2 \equiv \frac{\alpha_s RT}{c_s} \frac{P_s l_s}{P_a^2} \tag{29}$$

Since the diffusion permeabilities of the membrane layers have been estimated and the thickness of the support (which practically coincides with the thickness of the membrane as a whole) is easy to measure, from eq 29, one can determine the chemical capacity of the support. For coarse-porous supports, the chemical capacity is given by

$$\alpha_s \equiv \frac{c_s \gamma_s}{RT} \tag{30}$$

where γ_s is the support porosity, and thus, from Eq(29), we obtain

$$\gamma_s = \frac{t_0^* P_a^2}{l_s P_s} \tag{31}$$

The thickness of the membrane was 160 μm. For the porosity of the support, we have obtained the values listed in Table 3. Finally, by using this definition

$$P_s \equiv \frac{\gamma_s D_s}{l_s} \tag{32}$$

we could estimate the salt diffusion coefficient inside the support pores, D_s (also listed in Table 3). With a bulk salt diffusion coefficient of approximately 2×10^{-9} m^2/s, this yields a tortuosity factor of 2.7−3.2. In view of a porosity of 10−11%, that value appears to be reasonable. It is also remarkable that the estimated values of the support porosity turn out practically independent of the salt concentration. That confirms the correctness of our assumption that the support properties may be considered the same for all of the concentrations studied.

To conclude, let us estimate a posteriori the values of the parameter r, which was assumed to be sufficiently large in the interpretation of transients of the transmembrane potential. According to the definition of eq 14, to do so we need to know the specific chemical capacities and the diffusion permeabilities of both membrane layers. Those properties of support have been estimated above. For the active layer, we can only determine the specific diffusion permeability (if the active layer thickness is known). Nevertheless, the information that we have enables us to make at least some reasonable estimates of the parameter r. Indeed, from the definition of the chemical capacity of eq 2, one can obtain this approximate relationship

$$\alpha_a \approx \frac{c_s \gamma_a \Gamma_a}{RT} \tag{33}$$

where γ_a is the porosity of the active layer and Γ_a is the distribution coefficient of co-ions between the active layer pores and the equilibrium solution. By using that relationship, for the parameter r we obtain

$$r^2 \approx \frac{1}{\gamma_a \Gamma_a} \frac{\gamma_s}{\rho} \frac{l_s}{l_a} \tag{34}$$

By using the values listed in Table 3 and assuming $l_a \approx 1$ μm, for example, in the 0.03 M solution we obtain $r \approx (1.6/\sqrt{\gamma_a \Gamma_a})$. The information on the thermodynamic properties of active layers of composite or asymmetric membranes is difficult to obtain because of the very small contribution of the active layers to the total membrane volume. Nevertheless, for very rough estimates, we may make use of the available information on the active layer diffusion permeability. Indeed, since

$$P_a l_a = \gamma_a \Gamma_a D_a \tag{35}$$

we can estimate the product of the sought-for parameter combination and of the effective diffusion coefficient in the "pores" of support. Again, in the 0.03 M solution, by assuming $l_a \approx 1\mu$m, we obtain $\gamma_a \Gamma_a D_a \approx 2.4 \times 10^{-12}$ m^2/s. That value is almost 3 orders of magnitude smaller than the bulk diffusion coefficient of KCl. In our opinion, it is highly improbable that the whole of that difference may be ascribed to the effective diffusion coefficient alone. Thus, the product $\gamma_a \Gamma_a$ appears to be essentially smaller than 1 and the parameter r essentially larger than 1.6. It is easy to show that in the more dilute solutions, the values of the parameter r are still larger. Thus, our use of the limiting case of $r \rightarrow \infty$ in the interpretation of transients of the transmembrane potential appears to be justified.

Conclusions

The chronopotentiometry after current switch-off enables one to single out the component of the transmembrane electric potential difference due to the direct current concentration polarization of the interface between supported thin nanoporous layers and their supports. That is especially useful in the case of bilayer systems whose supports have relatively high ohmic resistances (for example, nanofiltration membranes).

The measurements carried out with a commercial nanofiltration membrane have revealed that the technique can yield quite reproducible results especially in not too dilute electrolyte solutions. It has been shown that the method is especially informative if used in combination with detailed filtration measurements as well as with the measurements of steady-state membrane potential or of membrane diffusion permeability. Sample estimates have enabled us to conclude that in a 0.03 M KCl solution of pH 5.6 the principal rejection mechanism of the Desal5 DK membrane is not directly related to the fixed electric charge. That conclusion has been confirmed by the estimates of the dependencies on the salt concentration of the ion transport numbers in the active layer and of its diffusion permeability. A quantitative comparison of time transients with the linear non-steady-state theory has enabled us to determine the characteristic relaxation times. From them, we could estimate the porosity of the support as well as the salt diffusion coefficient there, which yielded reasonable values practically independent

of salt concentration. That confirms the self-consistency of our interpretation.

Acknowledgment. We thank Fonds zur Förderung der wissenschaftlichen Forschung, Austria, for the financial support within the scope of research project P13978, "Non-Steady-State Methods of Membrane Characterization". We also thank G. Kellner and H. Leodolter for the valuable technical assistance.

List of Symbols

a = semiempirical parameter

$b \equiv \beta_s h$ = parameter defined by eq 15

c_s = salt concentration

$D_{a,s}$ = salt diffusion coefficient in the pores of active layer, support

E_m = membrane potential

E_{mi} = initial transient membrane potential

E_{ms} = steady-state membrane potential

$\tilde{E}_m \equiv FE_m/RT$ = dimensionless membrane potential

F = Faraday constant

$f_i(\xi,\omega)$ = Fourier transform of distribution of salt chemical potential within the ith layer

h = dimensionless support thickness

$I(\tau)$ = time-dependent density of polarizing current

$I(\omega)$= Fourier transform of time-dependent density of polarizing current

I_0 = amplitude of time-dependent density of polarizing current

$\tilde{I} \equiv I/2Fc_s$ = reduced current density

l_a = thickness of nanoporous (active) layer

P_a, P_s, P_m= molar diffusion permeability of nanoporous (active) layer, support, membrane

q_s = quantity of salt per unit volume (from the definition of chemical capacity)

r = parameter defined by eq 14

R = universal gas constant

$R(\omega)$ = spectral density of difference of salt chemical potentials across the active layer

T = absolute temperature

t = time

t_0 = characteristic relaxation time defined by eq 2

$t_0^* \equiv t_0 r^2$ = characteristic relaxation time defined by eq 22

t_k = transport number of counterion within the kth layer

Greek Symbols

α_k = specific chemical capacity of kth layer

β_k = layer-specific coefficient defined by eq 3

Γ_i = distribution coefficient of the ith ion

$\Gamma_{a,s}$ = distribution coefficient of co-ions between the pores of the nanoporous layer (support) and an equilibrium electrolyte solution

γ_s = porosity of the support

Δt_1 = difference between the transport number of ion "1" in the nanoporous layer and support

μ = salt chemical potential

ξ = dimensionless transmembrane coordinate

ρ = ratio of diffusion permeabilities of active layer and support defined by eq 20

σ_s = salt reflection coefficient

τ = dimensionless time scaled on t_0 defined by eq 2

τ^* = dimensionless time scaled on t_0^* defined by eq 22

χ_k = specific diffusion permeability of the kth layer

ω = dimensionless circular frequency

References and Notes

(1) Yaroshchuk, A. E. *Desalination* **2002**, *149*, 423.
(2) Zholkovskij, E. K. In *Surface Chemistry and Electrochemistry of Membranes*; Sorensen, T. S., Ed.; Marcel Dekker: New York, 1998, p 793.
(3) Jamnik, J.; Maier, J. *Phys. Chem. Chem. Phys*. **2001**, *3*, 1668.
(4) Sistat, P.; Pourcelly, G. *J. Membr. Sci*. **1997**, *123*, 121.
(5) Kontturi, K.; Mafé, S.; Manzanares, J. A.; Sundholm, G.; Vapola, R. *Electrochim. Acta* **1997**, *42*, 2569.
(6) Wilhelm, F. G.; van der Vegt, N. F. A.; Wessling, M.; Strathmann, H. *J. Electroanal. Chem.* **2001**, *502*, 152.
(7) Wilhelm, F. G.; van der Vegt, N. F. A.; Strathmann, H.; Wessling, M. *J. Appl. Electrochem*. **2002**, *32*, 455.
(8) Yaroshchuk, A. E.; Ribitsch, V. *Chem. Eng. J*. **2000**, *80*, 203.
(9) This difference is equal in absolute value and opposite in sign to the chemical potential difference across the support.
(10) Remember that we consider the times much longer than the characteristic Maxwell−Wagner relaxation time. Therefore even under non-steady-state conditions the electric current is continuous.
(11) For the counterions, the distribution coefficient is large. However, the second term in parentheses is negative in this case and can be shown to compensate the first one almost exactly.
(12) Some estimates of this parameter are carried out below a posteriori.
(13) Yaroshchuk, A. E.; Makovetskiy, A. L.; Boiko, Yu. P.; Galinker, E. W. *J. Membr. Sci*. **2000**, *172*, 203.
(14) Krol, J. J.; Wessling, M.; Strathmann, H. *J. Membr. Sci*. **1999**, *162*, 145.
(15) It is supposed that the ion transport numbers in the coarse-porous support are equal to the bulk ones.
(16) Yaroshchuk, A. E. *J. Membr. Sci*. **2002**, *198*, 285.
(17) Boiko, Yu. P.; Makovetskiy, A. L. Personal communication, 2002.
(18) Yaroshchuk, A. E. *Adv. Colloid Interface Sci*. **2000**, *85*, 193.